Spatial and Temporal Dynamics of *Phytophthora* Epidemics in Commercial Bell Pepper Fields

Jean B. Ristaino, Robert P. Larkin, and C. Lee Campbell

Associate professor, postdoctoral research associate, and professor, respectively, Department of Plant Pathology, North Carolina State University, Raleigh 27695-7616.

Funded in part by grant 92-37303-7715 from the National Research Initiatives Competitive Grants Program of the USDA.

We thank Greg Parra and Charles Harper for their careful technical assistance and D.-J. Van der Gaag, A. Pedroza-Sandoval, and S. Potter for their assistance in data collection and analysis. The statistical advice of Marcia Gumpertz is appreciated.

Accepted for publication 16 August 1993.

ABSTRACT

Ristaino, J. B., Larkin, R. P., and Campbell, C. L. 1993. Spatial and temporal dynamics of *Phytophthora* epidemics in commercial bell pepper fields. Phytopathology 83:1312-1320.

Epidemics in bell pepper caused by *Phytophthora capsici* were monitored in three commercial fields to characterize the spatial pattern of disease and to gain a preliminary indication of dispersal mechanisms that may influence spatial disease progress. Disease incidence increased from 3.8 to 35.8% and from 13.6 to 38.5%, and the final percentage of quadrats with plants with wilt, crown lesions, stem lesions, or dead plants was 15.8, 16.8, 15.5, and 15.3 in field one and 16.5, 23.5, 10.5, and 31 in field two, respectively. In field three, disease incidence increased from 15.9 to 22.6% in the upper portion of the field and from 53.1 to 67.3% in the lower portion of the field. Based on ordinary runs analysis, rows with aggregated patterns of diseased plants within rows ranged from 15 to 35, 30 to 50, 10 to 20, and 77 to 85% over the season in fields one, two, and the upper and lower portions of field three, respectively. Rows with aggregated patterns of disease across rows ranged from 5 to 30, 20 to 70, 31 to 32.5, and 62 to 74% over the season in fields one, two, and the upper and lower portions of field three, respectively. Two-dimensional distance class analysis also indicated nonrandom spatial patterns as well as greater spread of disease within rows than across rows in fields one and two. In field one, minimum core cluster size increased from 4 to 68 distance class units as several small reflected core clusters coalesced over time within and across several rows of the field. In field two, minimum core cluster size increased from 26 to 35 distance class units, whereas a single reflected core cluster increased in size from 5 to 39 distance class units. The core and reflected core clusters in field two did not coalesce over time, and an average intercluster distance of four rows was observed. In field three, a single large core cluster dominated the lower portion of the field and ranged in size from 350 to 366 distance class units. Across-row spread of disease was predominant in the lower portion of field three and coincided with a low drainage area where water flowed across plant rows. In the upper portion of field three, a large core cluster and several reflected core clusters expanded predominantly within rows, and an average intercluster distance of 23 rows was observed at the last disease assessment date. Incidence of quadrats with plants with stem lesions lagged behind the incidence of quadrats with plants with wilt or crown lesions in all fields, whereas plants with leaf or fruit lesions were not observed. Infection of roots by the pathogen and subsequent spread of the disease from roots to the crown of the plant was the predominant mode of infection. Dispersal of inoculum apparently occurred within rows in surface water in these fields, and secondary spread of the pathogen from plant to plant was evident.

Patterns of disease are the integration of initial patterns of propagules and the subsequent processes of pathogen dispersal and host infection that occur during epidemic ontogeny. Spatial patterns of plants infected by primarily monocyclic, soilborne pathogens, such as *Macrophomina phaseolina* on *Euphorbia lathyris* (12) and *Peronosclerospora sorghi* on sorghum (26), initially reflect the pattern of inoculum in soil, and the integrity of this pattern is maintained during epidemic development within a cropping season. For other pathogens, such as *Phymatotrichum omnivorum* on cotton (9) and *Sclerotium rolfsii* on peanut (24) or carrot (27), spatial patterns initially reflect propagule patterns; however, as mycelium grows through or across soil, initial disease foci enlarge and may coalesce. For many diseases caused by *Phytophthora* species, the pathogen is polycyclic within a growing season and can be dispersed in water through soil, down rows in irrigation or rain water, or by splashing (1,2,13,19–22,25). The pattern of diseased plants will change over time and will reflect the initial inoculum pattern and the mechanisms of inoculum dispersal that are in operation.

The challenge of contemporary work on spatial pattern of plant diseases is to move beyond the simple description of the pattern of inoculum or disease at a single point in time and into the analytical or explanatory phases of spatial pattern analysis. Many methods of spatial pattern analysis do not take into account the actual location of the sample site in the field (16), which results in a loss of valuable information in the analysis. If the mode(s) of dispersal of a pathogen and the environmental conditions required for dispersal are known and the spatial coordinates of the data are utilized in the analysis, changes in spatial pattern can lead us to rule out certain dispersal and infection processes and provide confirmatory evidence for others. For example, changes from a random to an aggregated pattern, as well as changes in cluster number, size, and orientation or in intercluster distance may reflect the operation of specific spatial processes.

A critical factor in moving from descriptive to analytical or explanatory spatial studies of plant disease epidemics is the appropriate and innovative interpretation of the results with available, analytical techniques. The methods of spatial pattern analysis and applications of these methods in plant disease epidemiology have been reviewed (3). Spatial pattern analysis can be based on the position of healthy or diseased plants or pathogen propagules within a row or series of rows (11), quadrat or plot count data (9), or distance measurements between diseased or healthy plants (6,15,18). Distance-based methods of spatial pattern analysis have been used extensively in ecological studies (4,17) and have been used only recently in studies of the spatial processes of plant disease epidemics (5,7,14).

Proctor (18) described a distance class method of studying clustering and anisotropy of tobacco mosaic virus-infected plants in 4- × 5-lattice patches of plants. Gray et al (6) modified the technique used to characterize clustering of diseased plants within any size lattice. Muskmelon plants infected with watermelon mosaic virus 2 occurred in clusters, and the degree of clustering was affected by host genotype (7). Rhizoctonia web blight was spatially aggregated within rows, across rows, and diagonally in container-grown azalea (5). Nelson et al (15) developed a PC-based version of Gray's (6) two-dimensional distance class analysis procedure and used the analysis to quantitatively compare the

spatial patterns of a complex of virus diseases and fungal and bacterial leaf spot diseases on white clover. Virus-susceptible white clover had more numerous and larger clusters of disease than did virus-resistant germ plasm (14). Fields with splash-dispersed leaf spot pathogens exhibited significant edge effects and large clusters of diseased plants, whereas fields with aerially dispersed leaf spot pathogens exhibited smaller clusters in the interior of the plots of white clover (14).

In this study, we used two-dimensional distance class analysis and ordinary runs analysis in two directions to quantify the changes in spatial pattern of disease caused by *Phytophthora capsici* Leonian in three bell pepper fields infested with natural inoculum of the pathogen and managed as commercial production fields. Our goal was to characterize the spatial pattern of *Phytophthora* epidemics in grower-managed fields and to gain a preliminary indication of dispersal mechanisms that may influence spatial disease progress.

MATERIALS AND METHODS

Experiments were conducted in three locations in commercial pepper (*Capsicum annuum* L.) fields in which the soil was infested naturally with inoculum of *P. capsici*. Fields were located in the coastal plain region of North Carolina. Fields one and two were adjacent fields, whereas field three was located approximately 8 km away. Soil textures, determined by mechanical analysis (8), were similar among fields, and soils were classified as sandy loam (76% sand, 6% silt, 18% clay), sandy clay loam (73% sand, 7% silt, 20% clay), and sandy loam (75% sand, 8% silt, 17% clay) in fields one, two, and three, respectively. In each field, the presence of *P. capsici* was confirmed by isolations from characteristic crown, root, and stem lesions on Phytophthora selective medium (PARPH) (10).

Fields were cultivated and prepared by growers, using standard cultural practices (23). Beds were shaped with 1 m between rows and planted with a single row of plants per bed. Transplanting equipment did not permit individual plants to be established in regular, equally spaced lattices within the fields. Thus, data were collected from contiguous quadrats that contained two to three transplants of the susceptible pepper cultivar Jupiter. Within-row plant spacing was approximately 30 cm. In fields one and two, 20 rows were divided into 20 quadrats, each approximately 1 m^2 (400 quadrats each). In field three, 40 rows were divided into 70 quadrats, each approximately 1 m^2. Data from field three were analyzed separately for the upper portion and the lower portion of the field (1,400 quadrats each), because a cluster of high disease incidence dominated the lower portion of the field.

Incidence of disease on individual plants within quadrats was assessed nine times in field one, 10 times in field two, and three times in field three. Disease-symptom types included plants with wilt without lesions, with crown lesions, with stem lesions above the soil line, with fruit lesions, with leaf lesions, and dead plants. Disease incidence was calculated as the percentage of quadrats with at least one diseased plant. Disease incidence data were mapped at each assessment date for each field. Disease incidence over time was plotted by symptom type for fields one and two. Regression analysis was used with the linear model $y = b_0 + b_1 t$, in which y is percent disease incidence and t is time expressed as day of the year, to compare the slopes of the lines with the Statistical Analysis System (SAS Institute, Cary, NC). This model provided a good fit for the observed data.

Ordinary runs analysis was conducted within and across rows on disease incidence data for each row or column separately and calculated by quadrats at each disease assessment date (9,11). Runs analysis also was conducted within each row on disease incidence data collected on individual plants at each disease assessment date. The percentage of rows with clustered patterns of disease was calculated, and the location of rows with clustered patterns of disease was noted.

Two-dimensional distance class analysis (6) was used to characterize the spatial arrangement of diseased and healthy plants within quadrats with 2DCLASS software (15). All possible pairs of quadrats containing infected plants within the lattice of contiguous quadrats were identified and assigned an $[X, Y]$ distance class, in which X is the row designation and Y is the across-row designation in the field. X and Y correspond to the columns and rows shown in the distance class matrices. The $[X, Y]$ distance class designation does not identify the position of infected quadrats in the lattice but refers to the absolute distance between quadrats within a pair (6). The number of pairs of quadrats containing infected plants occurring in each $[X, Y]$ distance class was standardized by dividing by the total number of pairs of quadrats containing living plants occurring in the same $[X, Y]$ distance class. The observed standardized count frequency (SCF) is a dimensionless number that represents the frequency of occurrence of pairs of quadrats containing infected plants in that $[X, Y]$ distance class relative to the number of pairs of quadrats containing infected plants in all other distance classes in the lattice (6). Comparison of observed and expected SCFs ($P \leq 0.05$) in each $[X, Y]$ distance class was used to define and quantify the randomness of pairs of quadrats containing diseased plants and their orientation in the lattice. The minimum percentage of SCFs needed to indicate nonrandomness was 5–10% of the total distance classes. Expected SCFs were determined by 400 computer simulations with a pseudorandom function and assigning the same number of quadrats containing infected plants randomly within a lattice of the same dimension. The analysis was conducted separately on spatial data from each assessment time in each field.

The minimum core cluster size was defined as the number of significant and adjacent $[X, Y]$ distance classes (including the $[X, Y]$ distance class [0,0]) that formed a discrete, contiguous group in the upper left corner of the distance class matrix. Minimum reflected core cluster size was defined as the number of significant and adjacent $[X, Y]$ distance classes that form discrete, contiguous groups elsewhere in the two-dimensional distance class matrix. Minimum cluster number was defined as the number of contiguous groups of significant $[X, Y]$ distance classes within the distance class matrix. If only n reflected clusters are evident in the two-dimensional distance class matrix and no core cluster is present, then the minimum number of clusters is $n + 1$, because groups of SCFs within the two-dimensional distance class matrix are reflections of at least one additional cluster in the data set (15). A cluster was counted if two or more SCFs were adjacent in an $[X, Y]$ distance class. The number and size of reflected core clusters was tabulated. Cluster shape was defined as the shape of the contiguous groups comprising minimum core and minimum reflected core clusters. Within- and across-row effects were interpreted as the greatest number of significant, adjacent SCFs detected in any $[X]$ or $[Y]$ distance class. For within- and across-row effects adjacent to the $[X, Y]$ distance class [0,0], a value of one was added to the total number of adjacent, significant SCFs.

Edge effects were interpreted as significant if more than 15–20% of the SCFs were significantly greater than expected in the outermost $[X, Y]$ distance classes [19,0–19] and [0–19,19] in both fields one and two. Significant edge effects were accepted in both the upper and lower portions of field three if more than 15–20% of the SCFs were significantly greater than expected in the $[X, Y]$ distance classes [39,0–34] and [0–39,34].

RESULTS

Disease-symptom types observed in all fields included plants with wilt without lesions, with crown lesions, with stem lesions, and dead plants, whereas no fruit or leaf lesions were observed on plants in any field. The symptoms of disease were confirmed to be due to infection by *P. capsici* by isolation of the pathogen from infected plants. Rainfall recorded at a nearby experiment station occurred on days 159, 164, 179, 205, and 221 when 2.8, 5.4, 3.9, 4.7, and 4.8 cm of rainfall occurred, respectively.

Incidence of quadrats in which disease occurred in field one increased from 3.8 to 35.8% over the season (Fig. 1A). The incidence of quadrats with plants with wilt symptoms, dead plants, and plants with crown lesions increased at rates of 0.38, 0.33,

and 0.27% per day, respectively ($r^2 = 0.95$, 0.97, and 0.27, respectively), in field one. However, the incidence of quadrats with plants with stem lesions lagged behind the incidence of quadrats with plants with other symptom types and increased after day 202 in field one at a rate of 0.23% per day ($r^2 = 0.47$) (Fig. 1A). Total disease incidence increased at a rate of 0.65% per day ($r^2 = 0.93$). The final percentage of quadrats with plants with wilt, crown lesions, stem lesions, or dead plants on day 211 was 15.8, 16.8, 15.5, and 15.3 in field one, respectively (Fig. 1A).

Disease incidence in field two increased from 13.6 to 38.5% over the season (Fig. 1B). The incidence of quadrats with plants with stem lesions also lagged behind the incidence of quadrats with plants with other symptom types in field two and did not increase until after day 202 at a rate of 0.19% per day ($r^2 = 0.71$) (Fig. 1B). Incidence of quadrats with dead plants, plants with wilt symptoms, and plants with crown lesions increased at rates of 0.42, 0.36 and 0.23% per day, respectively ($r^2 = 0.94$, 0.98, and 0.96, respectively), in field two. Final percentage of quadrats with plants with wilt, crown lesions, stem lesions, or dead plants was 16.5, 23.5, 10.5, and 31 in field two, respectively (Fig. 1B).

Incidence of quadrats with diseased plants in field three increased from 15.9 to 22.6% in the upper portion of the field and 53.1 to 67.3% in the lower portion of the field from day 209 to 223, respectively. In field three, the final percentage of quadrats with plants with wilt, crown lesions, stem lesions, or dead plants was 11.2, 7.4, 1.1, and 9.5, respectively, in the upper portion of the field and 19.1, 31.1, 6.5, and 42.4, respectively, in the lower portion of the field.

Runs analysis. In field one, three rows (15%) had aggregated within-row patterns of disease on all assessment dates until day 211 on which seven rows (35%) had aggregated within-row patterns of disease (Fig. 2A). Percentage of rows with aggregated within-row patterns of disease was higher in field two (Fig. 2B) than in field one (Fig. 2A) at all assessment times. In field two,

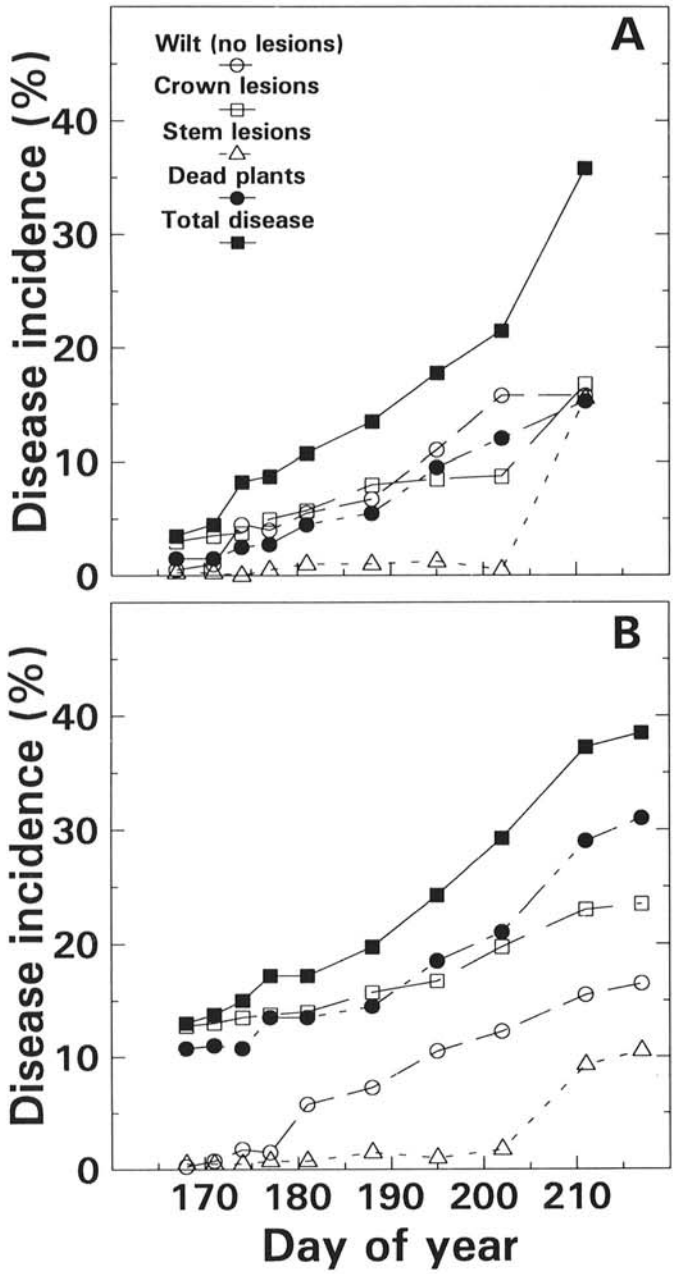

Fig. 1. Progression of *Phytophthora* epidemics caused by *Phytophthora capsici* in **A,** field one and **B,** field two. Disease incidence was calculated as the percentage of quadrats with at least one diseased plant with a different symptom type.

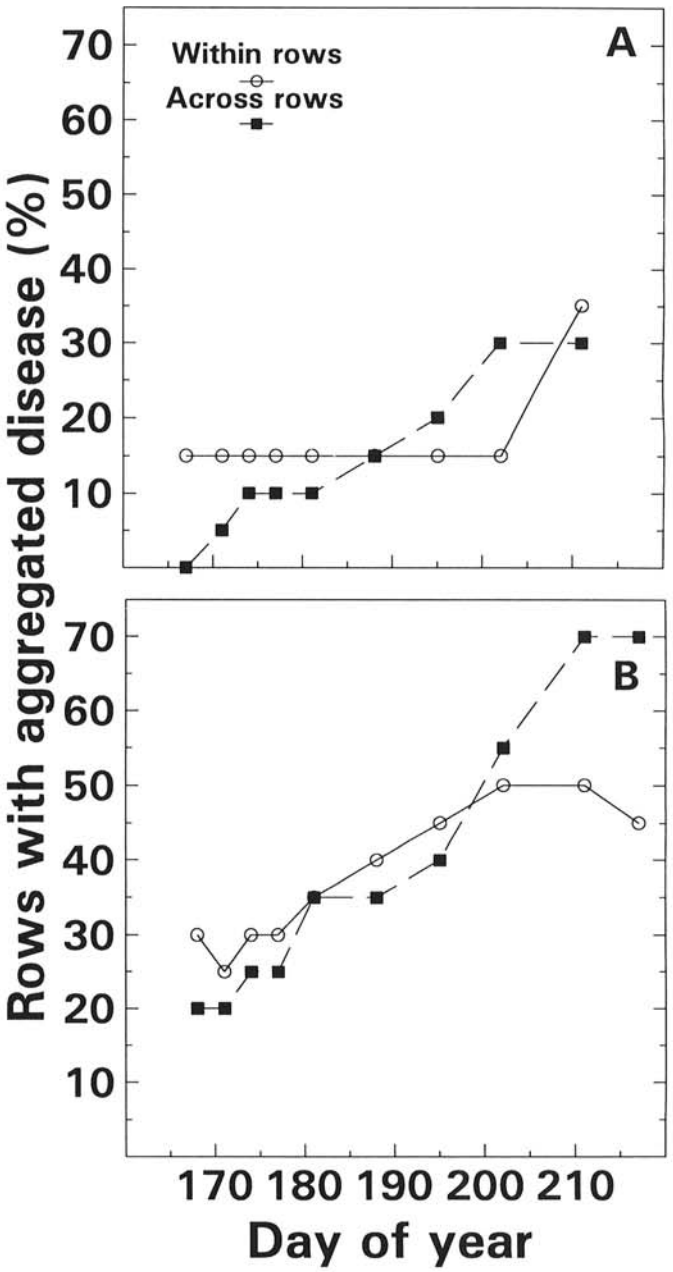

Fig. 2. Percentage of rows with aggregated patterns of disease caused by *Phytophthora capsici* over time as indicated by ordinary runs analysis in **A,** field one and **B,** field two.

percentage of rows with aggregated within-row patterns of disease ranged from 25 to 40 (5 to 8 rows) between days 168 and 188 but increased to 45 to 50 (9 to 10 rows) between days 195 and 217 (Fig. 2B). The percentage of rows with aggregated across-row patterns of disease ranged from 5 to 30 (1 to 6 rows) in field one (Fig. 2A) and 20 to 70 (4 to 14 rows) in field two (Fig. 2B) over time. In field one, aggregated across-row patterns of disease were lower than aggregated within-row patterns of disease between days 168 and 181, but the reverse was true on days 195 and 202 (Fig. 2A). In field two, the percentage of rows with aggregated across-row patterns of disease also was lower than the percentage of rows with aggregated within-rows patterns of disease at most disease assessment times, except on days 202, 211, and 217.

In field three, the percentage of rows with aggregated within-row patterns of disease was 10, 17.5, and 20 in the upper portion of the field and 77.5, 85, and 75 in the lower portion of the field on days 209, 216, and 223, respectively. The percentage of rows with aggregated across-row patterns of disease in field three was 31.4, 25.7, and 32.5 in the upper portion of the field and 74.3, 62.9, and 62.8 in the lower portion of the field at days 209, 216, and 223, respectively.

Two-dimensional distance class analysis. Significant, nonrandom distribution of pairs of quadrats with infected plants was observed at all disease assessment times in field one (Fig. 3A–H). Discrete, relatively isodiametric clusters of quadrats with diseased plants were observed in field one at day 167 (Fig. 3A). The minimum core cluster size was four and was evident from the higher than expected distribution of SCFs in the upper left corner of the $[X, Y]$ distance class matrix ([0,0–2] and [1,1]) (Fig. 3I). Minimum core cluster size increased from four to 68 (count includes [0,0] in the distance class matrix) by day 211 (Fig. 3I–P; Table 1). Cluster shape changed from isodiametric to elongate by day 174 (Fig. 3J). Total numbers of reflected core clusters ranged from five to three between days 167 and 177 (Fig. 3I–K) and decreased over time to one reflected core cluster by day 211

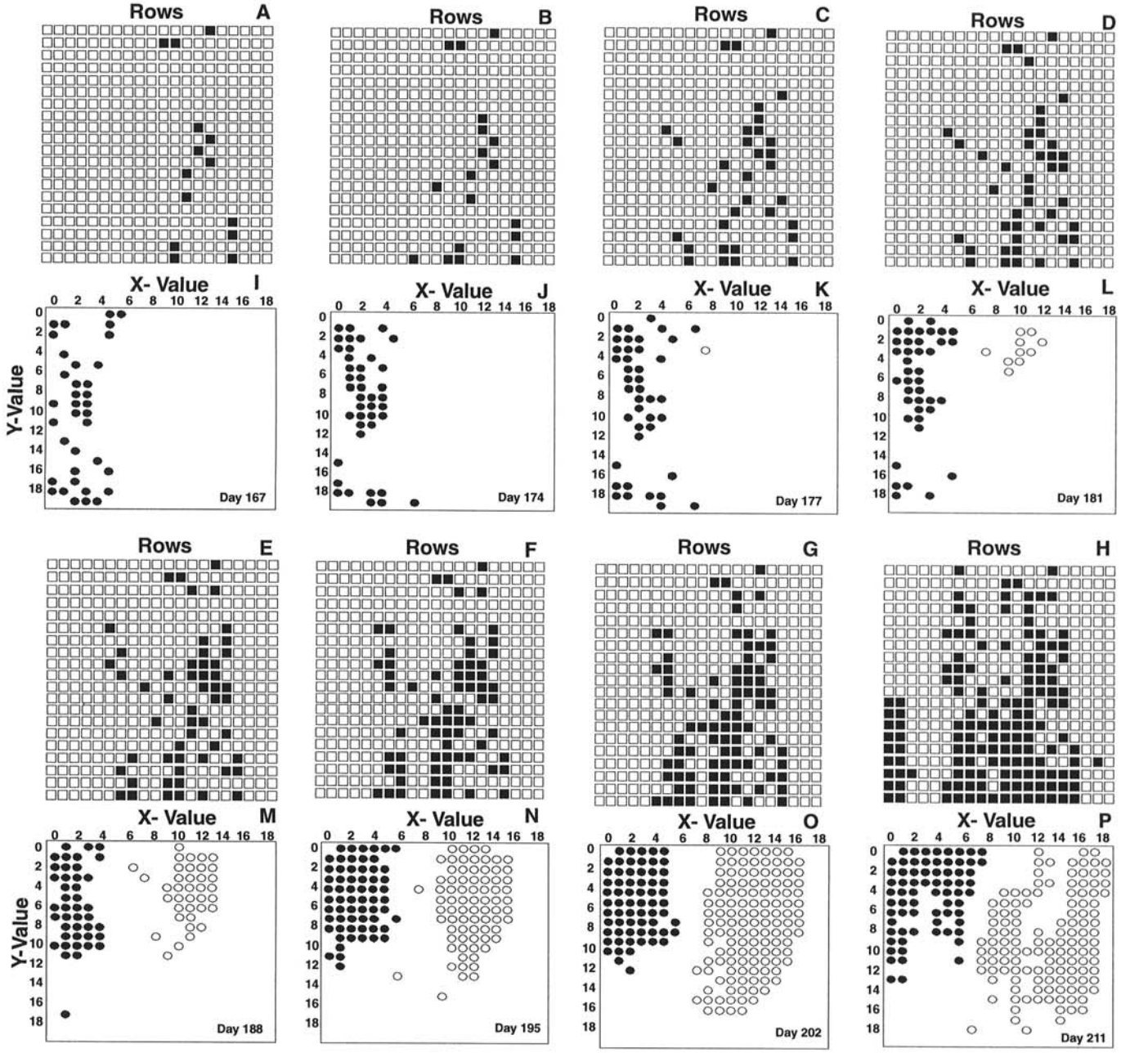

Fig. 3. A–H, Spatial pattern of *Phytophthora* epidemics in a 20-row × 20-column lattice of contiguous quadrats in field one and **I–P,** two-dimensional distance class analysis of the spatial pattern data in field one at days 167, 174, 177, 181, 188, 195, 202, and 211, respectively. Solid squares = quadrats that contain at least one diseased plant; open squares = quadrats that contain healthy plants. Solid circles = $[X, Y]$ distance classes with a standardized count frequency (SCF) greater than expected at $P \leq 0.05$; open circles = a SCF less than expected at $P \geq 0.95$.

(Fig. 3P) as several small reflected core clusters coalesced with the core cluster (Fig. 3I–P; Table 1). Fewer pairs of quadrats with infected plants occurred in the upper left corner of field one over time (Fig. 3A–H), as indicated by the increasing number of significantly lower SCFs in the X-value distance classes [9–19] between days 181 and 211 (open circles in Fig. 3L–P). This indicates that a large area of the field also contained pairs of quadrats with no diseased plants.

Aggregation of quadrats with diseased plants within rows was apparent over time in field one (Table 1; Fig. 3A–H). For example, $[X, Y]$ distance classes [3,7–11], [2,5–12], [1,1–7], [1,0–8], [1,0–11], [1,0–12], [1,0–11], and [0,0–11] (Fig. 3I–P) indicated significant within-row effects on days 167, 174, 177, 181, 188, 195, 202, and 211, respectively. Maximum disease spread within rows in field one increased from 5 to 12 distance class units over the season (Table 1). Other significant within-row effects also were apparent over time in other $[X, Y]$ distance classes shown in Fig. 3I–P. Aggregation of quadrats with diseased plants across rows also was apparent and increased over time in field one (Table 1). However, the number of SCFs greater than expected in $[X, Y]$ distance classes within rows was higher than the number of SCFs greater than expected in $[X, Y]$ distance classes across rows at each disease assessment time in field one (Table 1). Although quadrats with diseased plants were observed at opposite edges of the field, significant edge effects were not detected at any time during the season.

Significant, nonrandom distribution of pairs of quadrats with infected plants also were observed at all disease assessment times in field two (Fig. 4A–H). A large core cluster was evident in field two at the initial disease assessment time (day 168) (Fig. 4I) and was larger than the core cluster in field one (Fig. 3I). The minimum core cluster size was 26 and was evident from the distribution of SCFs greater than expected in the upper left corner of the matrix in $[X, Y]$ distance classes [0,1–5], [1,0–5], [2,0–4], [3,0–4], and [4,0–3] (Fig. 4I; Table 1). Minimum core cluster size increased from 26 to 35 distance class units (count includes [0,0] in the distance class matrix) by day 217 (Fig. 4I–P; Table 1). A distinct reflected core cluster was apparent initially at day 168 in $[X, Y]$ distance classes [10,0], [10,2], [11,1–2], and [12,2] (Fig. 4I). This reflected core cluster grew in size over time from 5 to 39 distance class units (Fig. 4I–P; Table 1). In field two, the average intercluster distance between the core and reflected cluster was five rows on day 168 (Fig. 4I) and four rows by day 217 (Fig. 4P). Fewer pairs of quadrats with infected plants occurred in two areas in field two across four rows and seven rows as indicated by the large number of significantly lower SCFs in the X-value distance classes [4–7] and [13–19] (open circles in Fig. 4P). Aggregation of quadrats with diseased plants within rows also was apparent over time in field two (Table 1). As in field one, the number of SCFs greater than expected in $[X, Y]$ distance classes within rows was higher than the number of SCFs greater than expected in $[X, Y]$ distance classes across rows at

TABLE 1. Spatial statistics from two-dimensional distance class analysis of disease incidence data from *Phytophthora* epidemics caused by natural inoculum of *Phytophthora capsici* in three commercial bell pepper fields

Day of year	Number of quadrats with diseased plants	SCF[a]		Minimum cluster size[b]		Total number of clusters	Effect[c]	
		+	−	Core	Reflected		Within row	Across row
Field 1								
167	14	36	0	4	2,2,4,10,12	6	5	3
171	18	41	0	24	3,13	3	6	4
174	33	41	0	31	2,3,4	4	8	4
177	35	41	1	27	3,3,4	4	7	3
181	43	40	10	35	3	2	9	6
188	54	42	37	42	0	1	12	5
195	71	62	76	63	0	1	13	6
202	86	65	126	66	0	1	12	7
211	143	70	128	68	2	2	12	9
Field 2								
168	52	30	26	26	5	2	6	5
171	55	33	25	25	2,5	3	6	5
174	60	39	36	26	14	2	6	6
177	61	41	41	27	15	2	6	6
181	70	42	49	31	11	2	8	5
188	80	53	80	35	2,17	3	8	6
195	98	55	86	30	26	2	7	6
202	119	59	119	28	32	2	8	5
211	151	75	158	35	41	2	12	5
217	155	73	154	35	39	2	12	5
Field 3, upper portion								
209	223	333	244	137	2,2,5,179	5	35	7
216	276	423	317	126	2,295	3	35	10
223	316	449	345	126	2,2,2,2,314	6	35	11
Field 3, lower portion								
209	743	349	964	350	0	1	17	23
216	844	361	952	362	0	1	17	24
223	942	365	937	366	0	1	17	24

[a] Number of $[X, Y]$ distance classes in which the observed standardized count frequency (SCF) was significantly greater (+) ($P < 0.05$) or less (−) than ($P > 0.95$) expected under a random spatial pattern.

[b] The minimum core cluster size was defined as the number of significant and adjacent $[X, Y]$ distance classes (including the $[X, Y]$ distance class, [0,0]) that formed a discrete, contiguous group in the upper left corner of the distance class matrix. Minimum reflected core cluster size was defined as the number of significant and adjacent $[X, Y]$ distance classes that form discrete, contiguous groups elsewhere in the two-dimensional distance class matrix. A cluster was counted if two or more SCFs were adjacent in the $[X, Y]$ distance class matrix.

[c] Within- and across-row effects were interpreted as the greatest number of significant, adjacent SCFs detected in any $[X]$ or $[Y]$ distance class. For within- and across-row effects adjacent to the $[X, Y]$ distance class [0,0], a value of one was added to the total number of adjacent, significant SCFs.

most disease assessment times in field two (Table 1). However, the higher within-row spread of disease in this field was due primarily to the expansion of the core cluster and a single reflected core cluster of quadrats with diseased plants (Fig. 4I–P) and not to the coalescence of many small reflected core clusters with the core cluster as in field one (Fig. 3I–P).

Significant, nonrandom patterns of quadrats with diseased plants also were observed in the upper portion (Fig. 5A–C) and the lower portion (Fig. 6A–C) of field three. Analysis of data from the upper portion of the field revealed core cluster sizes of 137–129 between days 209 and 223 (Table 1; Fig. 5D–F). A large reflected core cluster and several smaller reflected core clusters were observed between days 209 and 223 (Fig. 5D–F). Significant within-row effects also were apparent in the upper portion of field three (Table 1). Similar to fields one and two, the number of SCFs greater than expected in $[X, Y]$ distance classes within rows was higher than the number of SCFs greater than expected in $[X, Y]$ distance classes across rows at each disease assessment time in the upper portion of the field. This within-row effect was obscured when data from both the upper and lower portion of the field were combined and analyzed. Intercluster distance of approximately 23 rows was noted at the last assessment time (Fig. 5F).

A single, centrally located, large cluster of diseased quadrats dominated the lower portion of the field in field three (Fig. 6A–C). Minimum core cluster size increased from 350 to 366 distance class units from day 208 to 223 (Fig. 6D–F). No other clusters of diseased quadrats were observed in the lower portion of the field. In contrast to the upper portion of the field, the number of SCFs greater than expected in $[X, Y]$ distance classes across

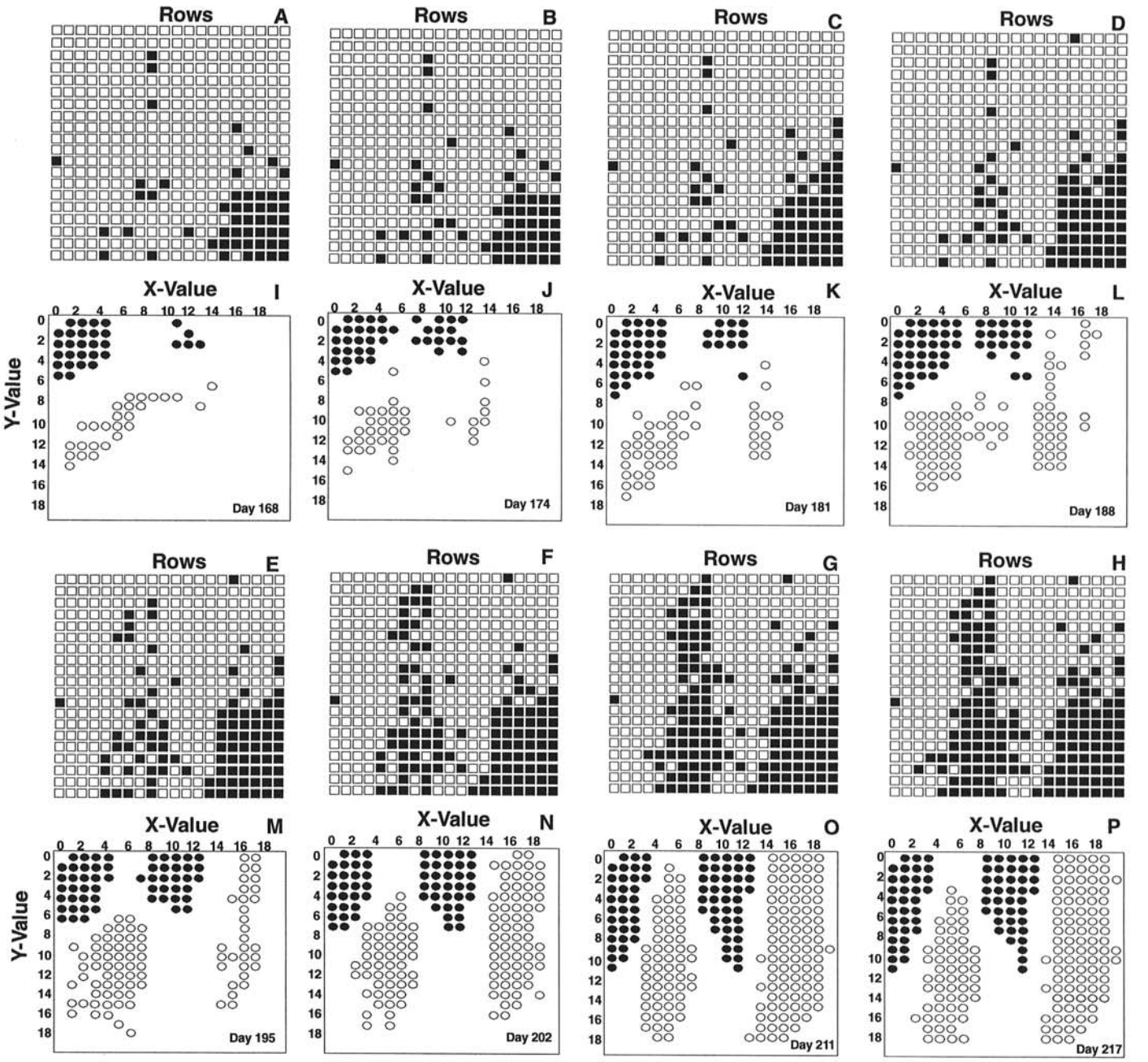

Fig. 4. A–H, Spatial pattern of *Phytophthora* epidemics in a 20-row × 20-column lattice of contiguous quadrats in field two and **I–P,** two-dimensional distance class analysis of the spatial pattern data in field two at days 168, 174, 181, 188, 195, 202, 211, and 217, respectively. Solid squares = quadrats that contain at least one diseased plant; open squares = quadrats that contain healthy plants. Solid circles = $[X, Y]$ distance classes with a standardized count frequency (SCF) greater than expected at $P \leq 0.05$; open circles = a SCF less than expected at $P \geq 0.95$.

rows was higher than the number of SCFs greater than expected in $[X, Y]$ distance classes within rows at each disease assessment time in the lower portion of field three (Table 1).

DISCUSSION

Distinctive spatial patterns of disease developed during *Phytophthora* epidemics in bell pepper in the three fields in our study in which natural inoculum of *P. capsici* was present. Nonrandom patterns of disease were evident at all assessment times. Additionally, distinctive changes in patterns of aggregation were observed over time.

Analysis of the data with ordinary runs analysis indicated that within-row aggregation of disease predominated early in epidemic development in fields one and two, whereas, late in the season, apparent across-row aggregation of disease was observed (Fig. 2). This increase in apparent across-row aggregation of disease late in the season was probably due to the simultaneous spread of disease within adjacent rows of plants. Disease spread within rows also was observed before disease spread across rows in a previous study of *Phytophthora* epidemics in Florida when point sources of inoculum were introduced into fumigated, plastic-mulched fields (1). In field three of our study, disease was evaluated at three times late in the season (days 209–223), and considerable spread of inoculum within and across rows already had occurred. Madden et al (11) considered ordinary runs analysis better than the original doublets or corrected doublets analyses for determination of randomness of infected plants within a field; however, there are limitations to the procedure (6). We used ordinary runs analysis as an initial exploratory technique to examine the percentage of rows with aggregated patterns of disease.

Disease incidence data from *Phytophthora* epidemics collected on a quadrat basis allowed us to utilize a two-dimensional distance class method that has been used only recently to characterize spatial patterns of epidemics in the field (5,7,14,18). The method quantitatively estimates randomness of infected plants, is tolerant of missing data, and allowed us the opportunity to describe quantitatively the size and location of clusters of quadrats with diseased plants and intercluster distance within the field (6). Two-dimensional distance class analysis is a useful tool for the analysis of binary data, and the spatial integrity of the data is not lost in the analysis. Thus, two-dimensional distance class analysis provided a robust procedure for analysis of the spatial characteristics of our data and allowed us to quantify cluster size, location, orientation, and intercluster distance in the fields. This analysis may be inappropriate when the proportion of infected plants is very small (<0.05) in relation to the total number of plants in the lattice (15), because all relevant distance classes tend to yield significant SCFs when disease proportion is low, even though diseased plants may be arranged randomly. In our data, disease proportion was lower than 0.05 in field one only at the first two assessment dates (days 167 and 171) but exceeded 0.05 thereafter. Thus, we believe this did not affect the interpretation of our results.

The two-dimensional distance class analysis revealed that aggregations of quadrats with infected plants occurred in distinct clusters in fields one and two. In field one, relatively isodiametric clusters of quadrats with diseased plants coalesced over time predominantly via within-row spread of the pathogen to form a single large core cluster in the lower center of the field by the end of the season. In field two, a large cluster was present initially in the lower right side of the field along with a single small cluster. These two clusters expanded predominantly within rows and did not coalesce to a great extent across rows as the epidemic progressed. In fact, many quadrats remained disease free in the upper portion of two large areas of both fields one and two at the end of the season (Figs. 3H and 4H).

The quantification of spatial pattern of disease over time is important to better understand underlying pathogen-dispersal

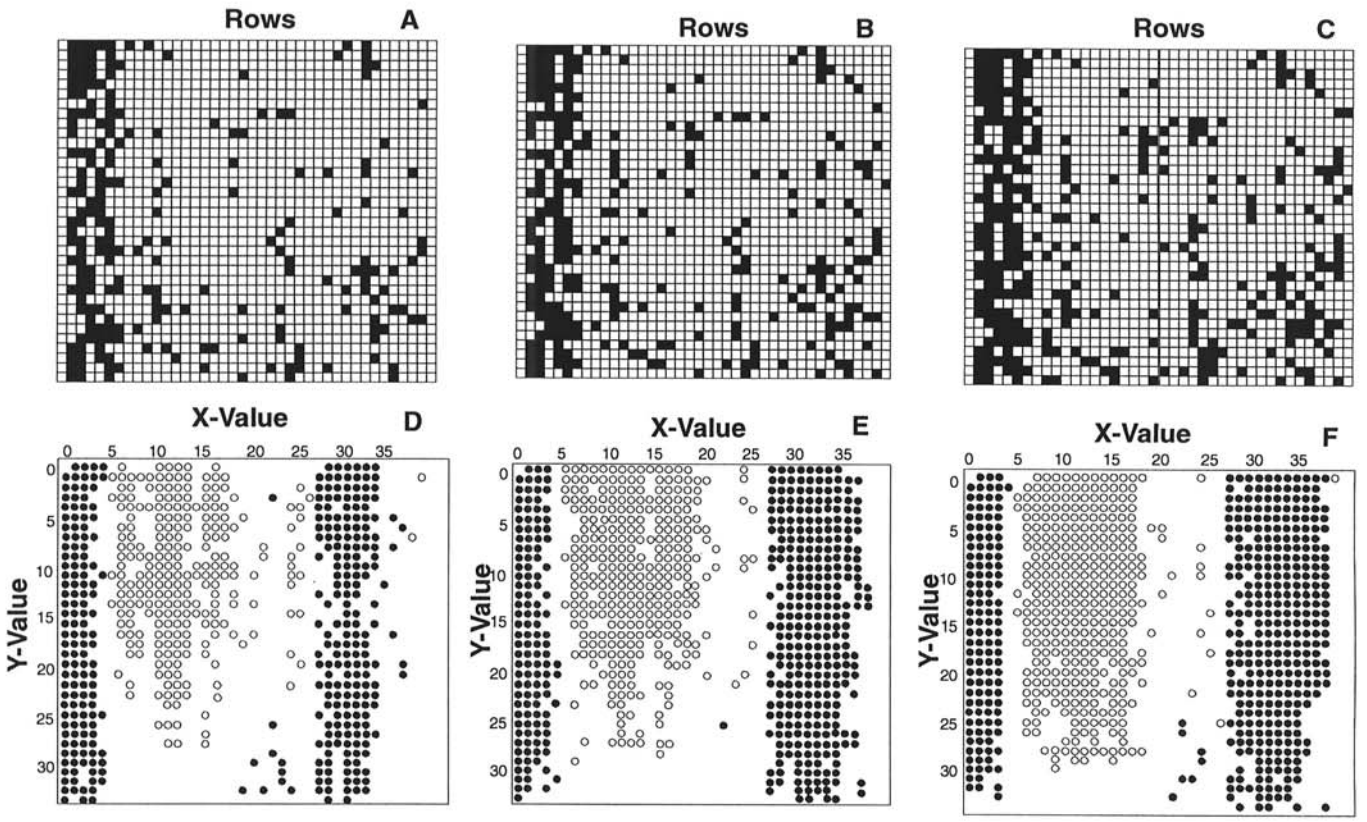

Fig. 5. A–C, Spatial pattern of *Phytophthora* epidemics in a 40-row × 35-column lattice of contiguous quadrats in the upper portion of field three and **D–F,** two-dimensional distance class analysis of the spatial pattern data in the upper portion of field three at days 209, 216, and 223, respectively. Solid squares = quadrats that contain at least one diseased plant; open squares = quadrats that contain healthy plants. Solid circles = $[X, Y]$ distance classes with a standardized count frequency (SCF) greater than expected at $P \leq 0.05$; open circles = a SCF less than expected at $P \geq 0.95$.

mechanisms. Overhead irrigation and rainfall probably contributed to the movement and spread of inoculum in the fields in our study. The predominance of within-row disease spread in fields one and two implies that the movement of surface water containing inoculum of the pathogen within the furrows was important. However, we did not sample water to confirm this hypothesis. Standing water also was observed to be "backed up" in the furrows at the ends of rows after rainfall and irrigations in fields one and two. Dispersal of inoculum of *P. parasitica* from introduced point sources has been demonstrated in furrows of processing tomato up to distances of 30 m down rows (13). In our study, inoculum may have been spread by an overhead irrigation rig as its moved within rows in fields one and two; however, the actual location of the irrigation rig was not noted in these fields. In field three, the large cluster of diseased plants in the lower portion of the field coincided with a low drainage area that occurred diagonally across the field from the upper right corner to the lower left corner of the field (Fig. 6A–C). Standing water across several rows was present in the lower portion of the field during initial disease observations. It was apparent that water flowed across plant rows during one or more rainfall events and that this accounted for the large across-row effect discerned with the two-dimensional distance class analysis in the lower portion of field three (Table 1).

Spatial pattern analysis of naturally occurring epidemics in the three fields in our study revealed significant amounts of within-row spread of disease. Strong across-row barrier effects have been demonstrated in leather rot epidemics caused by splash-dispersed introduced inoculum of *P. cactorum* on strawberry (20). Spread of *P. capsici* from point sources of introduced inoculum within and across rows of small plots has been described previously in pepper grown in fumigated soils in Florida and has been attributed to movement of inoculum on the surface of plastic with rainfall (1). We believe however, that our study is the first to demonstrate within- and across-row spread of disease in this pathosystem under commercial field conditions with natural inoculum of the pathogen.

The change in the incidence of various disease-symptom types over time in our study indicated that crown infection was the predominant symptom type. Wilting of plants in the absence of lesions generally preceded the observation of crown infections, indicating that infection of roots and subsequent spread of the pathogen to the crowns of plants was the predominant method of infection. Stem lesions above the soil surface on axial branches of the plants were observed rarely and occurred later in the season, whereas leaf and fruit infections did not occur at all, indicating that splash dispersal of soilborne inoculum to aerial parts of the plant was not important in these fields. We are in the process of further analyzing the spatial pattern of different symptom types over time under natural field conditions, in these and other fields, to elucidate and quantify the importance of dispersal mechanisms operating in this pathosystem and to devise cultural management strategies that will be effective in limiting pathogen dispersal.

LITERATURE CITED

1. Bowers, J. H., Sonoda, R. M., and Mitchell, D. J. 1990. Path coefficient analysis of the effect of rainfall variables on the epidemiology of Phytophthora blight of pepper caused by *Phytophthora capsici*. Phytopathology 80:1439-1446.
2. Campbell, C. L., Jacobi, W. R., Powell, N. T., and Main, C. E. 1984. Analysis of disease progression and the randomness of occurrence of infected plants during tobacco black shank epidemics. Phytopathology 74:230-235.
3. Campbell, C. L., and Madden, L. V. 1990. Spatial aspects of plant disease epidemics II: Analysis of spatial pattern. Pages 289-328 in: Introduction to Plant Disease Epidemiology. John Wiley & Sons,

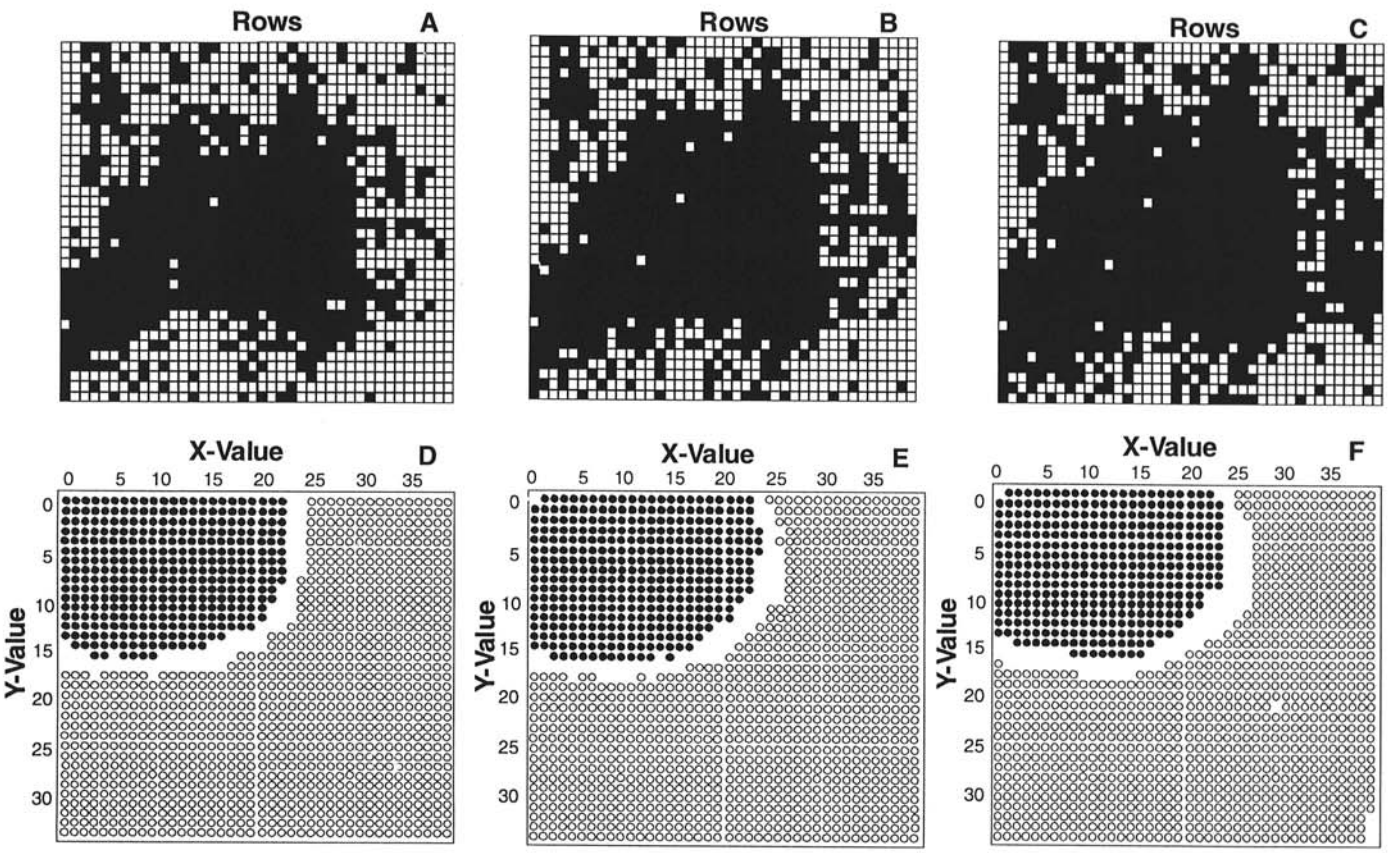

Fig. 6 A–C, Spatial pattern of *Phytophthora* epidemics in a 40-row × 35-column lattice of contiguous quadrats in the lower portion of field three and **D–F,** two-dimensional distance class analysis of the spatial pattern data in the lower portion of field three at days 209, 216, and 223, respectively. Solid squares = quadrats that contain at least one diseased plant; open squares = quadrats that contain healthy plants. Solid circles = $[X, Y]$ distance classes with a standardized count frequency (SCF) greater than expected at $P \leq 0.05$; open circles = a SCF less than expected at $P \geq 0.95$.

New York.
4. Clark, P. J., and Evans, F. C. 1954. Distance to nearest neighbor as a measure of spatial relationships in populations. Ecology 35:445-453.
5. Frisina, T. A., and Benson, D. M. 1989. Occurrence of binucleate *Rhizoctonia* spp. on azalea and spatial analysis of web blight in container-grown nursery stock. Plant Dis. 73:249-254.
6. Gray, S. M., Moyer, J. W., and Bloomfield, P. 1986. Two-dimensional distance class model for quantitative description of virus-infected plant distribution lattices. Phytopathology 76:243-248.
7. Gray, S. M., Moyer, J. W., Kennedy, G. G., and Campbell, C. L. 1986. Virus-suppression and aphid-resistance effects on spatial and temporal spread of watermelon mosaic virus 2. Phytopathology 76:1254-1259.
8. Hillel, D. 1982. Introduction to Soil Physics. Academic Press, New York. 365 pp.
9. Jeger, M. J., Kenerly, C. M., Gerik, T. J., and Koch, D. O. 1987. Spatial dynamics of Phymatotrichum root rot in row crops in the Blackland region of north central Texas. Phytopathology 77:1647-1656.
10. Kannwischer, M. E., and Mitchell, D. J. 1978. The influence of a fungicide on the epidemiology of black shank of tobacco. Phytopathology 68:1760-1765.
11. Madden, L. V., Louie, R., Abt, J. J., and Knoke, J. K. 1982. Evaluation of tests for randomness of infected plants. Phytopathology 72:195-198.
12. Mihail, J. D. 1989. *Macrophomina phaseolina*: Spatio-temporal dynamics of inoculum and of disease in a highly susceptible crop. Phytopathology 79:848-855.
13. Neher, D., and Duniway, J. M. 1992. Dispersal of *Phytophthora parasitica* in tomato fields by furrow irrigation. Plant Dis. 76:582-586.
14. Nelson, S. C., and Campbell, C. L. 1993. Comparative spatial analysis of foliar epidemics on white clover caused by viruses, fungi, and a bacterium. Phytopathology 83:288-301.
15. Nelson, S. C., Marsh, P. L., and Campbell, C. L. 1992. 2DCLASS, a two-dimensional distance class analysis software for the personal computer. Plant Dis. 76:427-432.
16. Nicot, P. C., Rouse, D. I., and Yandell, B. S. 1984. Comparison of statistical methods for studying spatial patterns of soilborne plant pathogens in the field. Phytopathology 74:1399-1402.
17. Pielou, E. C. 1969. An Introduction to Mathematical Ecology. John Wiley & Sons, New York. 358 pp.
18. Proctor, C. H. 1984. On the detection of clustering and anisotropy using binary data from a lattice patch. Commun. Statist.-Theor. Meth. 13:617-638.
19. Reynolds, K. M., Gold, H. J., Bruck, R. I., Benson, D. M., and Campbell, C. L. 1986. Simulation of the spread of *Phytophthora cinnamomi* causing a root rot of Fraser fir in nursery beds. Phytopathology 76:1190-1201.
20. Reynolds, K. M., Madden, L. V., and Ellis, M. A. 1988. Spatio-temporal analysis of epidemic development of leather rot of strawberry. Phytopathology 78:246-252.
21. Ristaino, J. B. 1991. Influence of rainfall, drip irrigation, and inoculum density on the development of Phytophthora root and crown rot epidemics and yield in bell pepper. Phytopathology 81:922-929.
22. Ristaino, J. B., Hord, M. J., and Gumpertz, M. L. 1992. Population densities of *Phytophthora capsici* in field soils related to drip irrigation, rainfall, and disease incidence. Plant Dis. 76:1017-1024.
23. Sanders, D. C., Averre, C. W., Sorenson, K. A., Estes, E. A., Beasley, E. O., and Bonanno, A. R. 1988. Commercial pepper production in North Carolina. N. C. Agric. Ext. Serv. Publ. 387. 16 pp.
24. Shew, B. B., Beute, M. K., and Campbell, C. L. 1984. Spatial pattern of southern stem rot caused by *Sclerotium rolfsii* in six North Carolina peanut fields. Phytopathology 74:730-735.
25. Shew, H. D. 1987. Effect of host resistance on spread of *Phytophthora parasitica* var. *nicotianae* and subsequent development of tobacco black shank under field conditions. Phytopathology 77:1090-1093.
26. Schuh, W., Jeger, M. J., and Frederiksen, R. A. 1988. Comparison of spatial patterns of oospores of *Peronosclerospora sorghi* in the soil and of sorghum plants with systemic downy mildew. Phytopathology 78:432-434.
27. Smith, V. L., Campbell, C. L, Jenkins, S. F., and Benson, D. M. 1988. Effects of host density and number of disease foci on epidemics of southern blight of processing carrot. Phytopathology 78:595-600.